

Magnetomechanical Properties and Anisotropy Compensation in Quaternary Rare Earth-Iron Materials of the Type $Tb_xDy_yHo_zFe_2$

S. C. Busbridge and A. R. Piercy
Department of Mathematical Sciences, University of Brighton
Lewes Road, Moulsecoomb, Brighton, BN2 4GJ, United Kingdom

Abstract — The static and dynamic magnetomechanical properties, in the temperature range $-60\text{ }^\circ\text{C}$ to $+100\text{ }^\circ\text{C}$, of quaternary compositions of the type $Tb_xDy_yHo_zFe_2$ ($x+y+z=1$) which have K_1 close to zero at $+20\text{ }^\circ\text{C}$ are presented. The maximum room temperature values of d_{33} (7.9 nm A^{-1}) and k_{33} (0.62) are achieved for $Tb_{0.20}Dy_{0.22}Ho_{0.58}Fe_2$, the composition for which K_2 is also close to zero at $+20\text{ }^\circ\text{C}$. Calculations performed with an anisotropy model including an eighth-order term show a 20 fold decrease in the anisotropy of $Tb_{0.20}Dy_{0.22}Ho_{0.58}Fe_2$ in comparison with Terfenol-D. This decrease is not as effective in improving material performance as the opposing influence of the reduction in saturation magnetostriction.

INTRODUCTION

The change in magnetomechanical properties of $Tb_{0.27}Dy_{0.73}Fe_2$ and $Tb_wHo_{1-w}Fe_2$ with variations in temperature and composition have been well characterised around the K_1 anisotropy compensation point [1, 2]. Interest in the $Tb_xDy_yHo_zFe_2$ ($x+y+z=1$) quaternary materials arises from the opposite sign of K_2 in $Tb_{0.27}Dy_{0.73}Fe_2$ and $Tb_wHo_{1-w}Fe_2$, thereby allowing suitable values of x , y and z to be found for which K_1 and K_2 are close to zero [3]. In this work we assess the effect of K_2 anisotropy compensation on the magnetomechanical properties of compositions for which K_1 is close to zero, and relate our findings to the easy axis of magnetisation [4].

EXPERIMENTAL

Magnetomechanical measurements were made on arc melted and vertical zone refined rods with nominal $\langle 112 \rangle$ orientation. Static measurements of the magnetostrain, λ , the magnetisation, M , and the bias field, H , were made by strain gauge, two coil induction and Hall effect techniques respectively. Measurements of the dynamic strain coefficient, d_{33} , and the dynamic susceptibility, χ_{33} , were made using lock-in techniques by applying a small alternating magnetic field of 400 A m^{-1} rms superimposed on H . The magnetomechanical coupling coefficient, k_{33} , was determined by the three-parameter method. All parameters were measured as a function of H , over the temperature range $-60\text{ }^\circ\text{C}$ to $+100\text{ }^\circ\text{C}$, on quaternary compositions for which K_1 was expected to be small at $+20\text{ }^\circ\text{C}$.

MAGNETOMECHANICAL PROPERTIES

Static Characteristics

Fig. 1 shows a plot of λ vs. bias field, H , for $Tb_{0.20}Dy_{0.22}Ho_{0.58}Fe_2$ at different constant temperatures. The general shape of the curves is common to all the compositions investigated and shows a tendency for the composition to become more difficult to saturate as the temperature is reduced. This arises because, with decreasing temperature, the easy direction of magnetisation changes from $\langle 111 \rangle$ at high temperatures to $\langle 100 \rangle$ at lower temperatures [4]. When $\langle 100 \rangle$ is easy, larger fields are required to rotate the magnetisation into the $\langle 112 \rangle$ applied field direction.

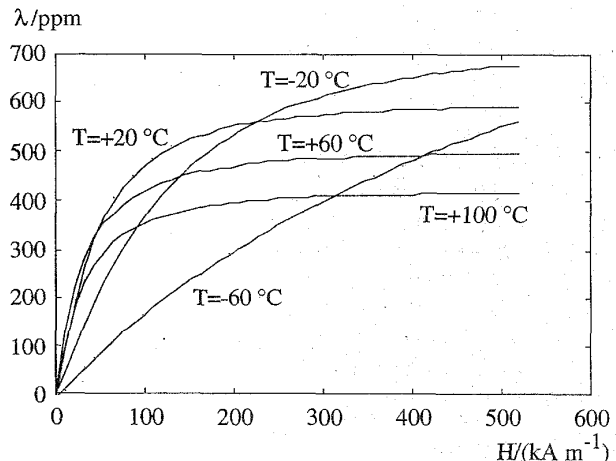


Fig. 1. λ vs. H for $Tb_{0.20}Dy_{0.22}Ho_{0.58}Fe_2$

The re-orientation of the magnetic moment also alters the shape of the curves of other static properties. As the temperature is reduced, the M vs. H curves indicate a higher static permeability at low values of bias field, followed by a sharper 'knee' and a slower approach to saturation at higher bias fields [1]. The normalised λ vs. M curves indicate that increasing H at low temperatures results in a higher fraction of saturation magnetisation, M_{sat} , being reached before significant strain is produced, followed by a more rapid approach to saturation via a much larger slope. These curves are shown in fig. 2 for $Tb_{0.20}Dy_{0.37}Ho_{0.43}Fe_{1.9}$ at different, constant, temperatures. We have previously related the details of these changes to the magnetisation process [5].

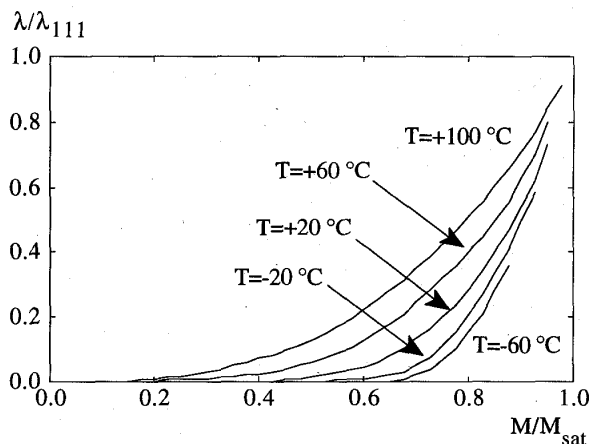


Fig. 2. Normalised λ vs. M for $\text{Tb}_{0.20}\text{Dy}_{0.37}\text{Ho}_{0.43}\text{Fe}_2$

Dynamic Characteristics

Fig. 3 shows a plot of d_{33} for $\text{Tb}_{0.20}\text{Dy}_{0.22}\text{Ho}_{0.58}\text{Fe}_2$ vs. H at different, constant, temperatures. d_{33} takes its maximum value of approximately 8 nm A^{-1} at a temperature of $+40^\circ\text{C}$ with an applied bias field of approximately 10 kA m^{-1} . For temperatures higher than $+40^\circ\text{C}$, the magnitude of d_{33} at any value of H decreases slightly due to the reduction in the saturation magnetostrain, λ_{sat} . For temperatures below $+40^\circ\text{C}$, the easy direction of magnetisation changes to $\langle 100 \rangle$ resulting in a dramatic reduction of d_{33} and a tendency for it to become almost independent of H . Similar curves have been recorded for k_{33} , with the largest value (0.62) being obtained for this composition at a temperature of $+40^\circ\text{C}$.

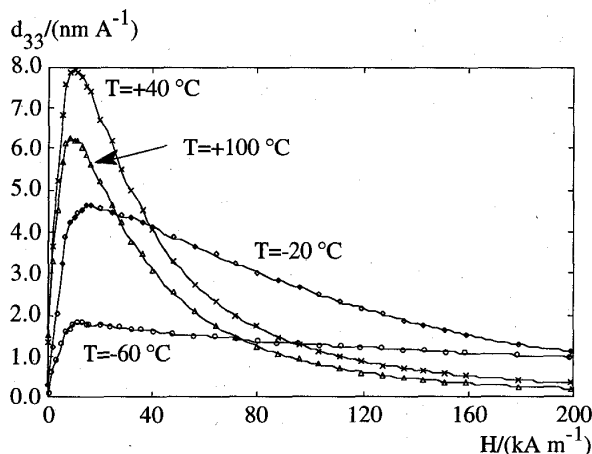


Fig. 3. d_{33} vs. H for $\text{Tb}_{0.20}\text{Dy}_{0.22}\text{Ho}_{0.58}\text{Fe}_2$

All of the compositions investigated displayed similar static and dynamic characteristics to those presented, and have much in common with the composition known as Terfenol-D

($\text{Tb}_{0.27}\text{Dy}_{0.73}\text{Fe}_2$). This similarity is attributable to the close proximity of the K_1 anisotropy point to room temperature.

The maximum value for d_{33} found for each composition is given in Table 1 together with the λ_{sat} and k_{33} values, all measured at $+20^\circ\text{C}$. The compositions are arranged in order of increasing Dy content, and all have K_1 close to zero at room temperature. The values of d_{33} and k_{33} for the quaternaries are greatest for those compositions for which K_2 is smallest [3], but are all disappointingly lower than the corresponding values for $\text{Tb}_{0.27}\text{Dy}_{0.73}\text{Fe}_2$. Also shown in Table 1 is the ratio $d_{33\text{max}}/\lambda_{\text{sat}}$ which gives the maximum value of d_{33} per unit of saturation magnetostrain (at $+20^\circ\text{C}$). This ratio does show a peak for the composition $\text{Tb}_{0.20}\text{Dy}_{0.22}\text{Ho}_{0.58}\text{Fe}_2$, which is nearest to the K_2 anisotropy compensation point.

Composition	λ_{sat}	max d_{33}	max k_{33}	$(d_{33\text{max}}/\lambda_{\text{sat}})$
x y z	$/10^{-6}$	$/\text{nm A}^{-1}$		$/(\text{nm A}^{-1} \times 10^3)$
0.13 0.00 0.87	320	2.8	0.30	8.8
0.20 0.22 0.58	640	7.9	0.62	12.3
0.23 0.26 0.51	900	6.2	0.46	6.9
0.20 0.37 0.43	680	4.4	0.36	6.5
0.27 0.73 0.00	1100	8.5	0.68	7.7

Table 1. Some Magnetomechanical Properties of $\text{Tb}_x\text{Dy}_y\text{Ho}_z\text{Fe}_2$ at $+20^\circ\text{C}$

We have additionally observed that the rate of change in the magnetomechanical properties with temperature (i.e. the rate at which the easy direction of magnetisation changes from $\langle 111 \rangle$ to $\langle 100 \rangle$ with decreasing temperature) reduces with increasing Dy content.

ANISOTROPY BEHAVIOUR

According to Atzmony and Dariel [6], the change in the easy direction of magnetisation with temperature can be understood by including an eighth-order anisotropy constant, K_3 , in the normal phenomenological equation for anisotropy energy, E_A :

$$E_A = K_0 + K_1(l^2m^2 + m^2n^2 + n^2l^2) + K_2(lmn)^2 + K_3(l^4m^4 + m^4n^4 + n^4l^4) \quad (1)$$

where l , m , and n are the usual direction cosines.

The results of their analysis, summarised in fig. 4, show the existence of stable $\langle 1uu \rangle$, $\langle 1u0 \rangle$ and $\langle 11u \rangle$ easy direction regions, as well as the more familiar $\langle 111 \rangle$, $\langle 100 \rangle$ and $\langle 110 \rangle$ regions. Our previous observations of the changes in the domain patterns of $\text{Tb}_{0.10}\text{Ho}_{0.90}\text{Fe}_{1.9}$ with temperature support the existence of a $\langle 1uu \rangle$ easy region [7]. This is consistent with the expected signs of K_2 and $K_3(>0)$; values of $\alpha_2 > 0$ (as in the case for $\text{Tb}_w\text{Ho}_{1-w}\text{Fe}_2$) requires the easy direction of magnetisation to change between $\langle 111 \rangle$ and $\langle 100 \rangle$

via $\langle 1uu \rangle$, or $\langle 110 \rangle$ and $\langle 1u0 \rangle$, or $\langle 11u \rangle$, $\langle 110 \rangle$ and $\langle 1u0 \rangle$. Values of $\alpha_2 < 0$ (as is the case for $\text{Tb}_{0.27}\text{Dy}_{0.73}\text{Fe}_2$) allow a much more direct transition between $\langle 111 \rangle$ and $\langle 100 \rangle$.

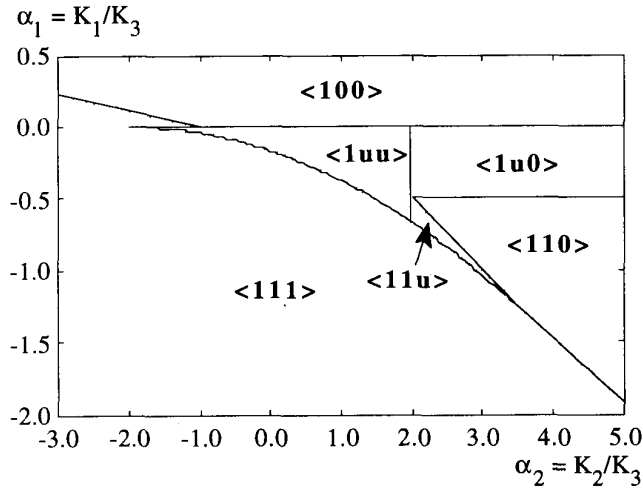


Fig. 4. Easy directions of magnetisation as given by equ. (1)

Now, if a composition is to be useful as a dynamic transducer, a large d_{33} and k_{33} are required. This implies that the easy direction of magnetisation should be $\langle 111 \rangle$, since $\lambda_{111} \gg \lambda_{100}$. Assuming our interpretation of the domain patterns to be correct, it follows that $\langle 111 \rangle$ will be easy provided that [6]:

$$\alpha_1 < \frac{-(\alpha_2 + 2)^2}{24} \quad (2)$$

In that case the energy required to overcome the anisotropy to change the direction of magnetisation from $\langle 111 \rangle$ to $\langle 112 \rangle$ (the axial direction of the rod-shaped samples), ΔE_A :

$$\frac{\Delta E_A}{K_3} = \frac{\alpha_2^2}{288} - \frac{\alpha_2}{216} + \frac{1}{432} \quad (3)$$

ΔE_A is plotted as a function of α_2 in fig. 5. We have taken $K_3 = +10^5 \text{ J m}^{-3}$ [6] and $-2 < \alpha_2 < +3$ (this is consistent with K_2 changing from $\sim +10^5 \text{ J m}^{-3}$ to -10^5 J m^{-3} as the composition changes with increasing Dy content from $\text{Tb}_{0.13}\text{Ho}_{0.87}\text{Fe}_2$ to $\text{Tb}_{0.27}\text{Dy}_{0.73}\text{Fe}_2$). ΔE_A exhibits a minimum when $\alpha_2 = 0.66$. It is interesting to note that the position of this minimum and the composition exhibiting the largest value of $d_{33}/\lambda_{\text{sat}}$ both occur on the Ho rich side of the composition lying mid-way between $\text{Tb}_{0.13}\text{Ho}_{0.87}\text{Fe}_2$ to $\text{Tb}_{0.27}\text{Dy}_{0.73}\text{Fe}_2$.

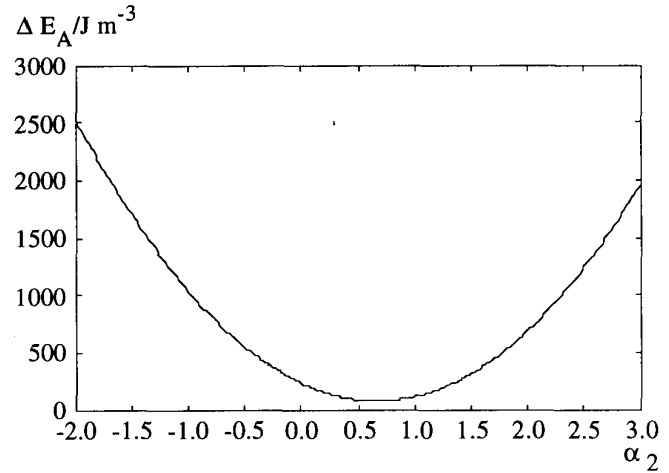


Fig. 5. ΔE_A plotted as a function of α_2 (equ. 3)

With ΔE_A dropping by a factor of about 20 over this composition range, it is surprising that there is not a corresponding increase in k_{33} . However, since the magnetomechanical energy required to saturate such materials is about 10^4 J m^{-3} , it appears that the effect of the reduction in anisotropy energy is less effective in increasing d_{33} and k_{33} than the opposing influence of the reduction in λ_{sat} .

REFERENCES

- [1] D. Kendall and A. R. Piercy, "Magnetisation Process and Temperature Dependence of the Magnetomechanical Properties of $\text{Tb}_{0.27}\text{Dy}_{0.73}\text{Fe}_{1.9}$ ", *IEEE Trans. Mag.*, vol. 26, pp. 1837-1839, Sept. 1990.
- [2] S. C. Busbridge and A. R. Piercy, "Magnetostriction and Magnetisation Processes in $\text{Tb}_x\text{Ho}_{1-x}\text{Fe}_{1.9}$ ", *J. Mag. Mag. Mat.*, 1994 (in print).
- [3] N. C. Koon, C. M. Williams and B. N. Das, "Giant Magnetostrictive Materials", *J. Mag. Mag. Mat.*, vol. 100, pp. 173-185, 1991.
- [4] U. Atzmony, M. P. Dariel et al., "Spin-Orientation Diagrams and Magnetic Anisotropy of Rare-Earth-Iron Ternary Cubic Laves Compounds", *Phys. Rev. B*, vol. 7, pp. 4220-4232, May 1973.
- [5] A. R. Piercy, S. C. Busbridge and D. Kendall, "Application of the Ratio d/χ to the Investigation of Magnetisation Processes in Giant-Magnetostrictive Materials", *J. Appl. Phys.*, vol. 76, pp. 7006-7008, Nov. 1994.
- [6] U. Atzmony and M. P. Dariel, "Nonmajor Cubic Symmetry Axes of Easy Magnetisation in Rare-Earth-Iron Laves Compounds", *Phys. Rev. B*, vol. 13, pp. 4006-4014, May 1976.
- [7] S. C. Busbridge and A. R. Piercy, "Domain Configurations in the Giant Magnetostrictive $\text{Tb}_x\text{Ho}_{1-x}\text{Fe}_{1.9}$ System in Different Easy Axis Regimes", *J. Appl. Phys.*, vol. 73, pp. 5354-5356, May 1993.